Jordanian Journal of Engineering and Chemical Industries

Print ISSN: 2616 - 9584 Online ISSN: 2617 - 720X

CO_2 Capture Using a Citric Acid and N-Methylmorpholine Deep Eutectic Solvent: A Computational Study

Bara' K. Al-Mahameed*[1]

[1]Al-Balqa Applied University, Maan University College, Department of Technological Sciences, Maan, Jordan

Highlights

- Citric acid and N-Methylmorpholine form stable and efficient DESs.
- DESs studied as novel solvents for CO_2 capture.
- Diffusion coefficient of CO_2 in DES is 4.879×10^{-12} m^2/s.

Abstract

In recent years, scientists and researchers have been interested in developing effective methods to reduce atmospheric CO_2 levels, due to their negative effects on the environment and human health. Deep eutectic solvents are considered promising alternatives for the future due to their attractive and distinctive properties. In this study, the citric acid and N-methylmorpholine were mixed to obtain a novel DES by forming a hydrogen bond between two components. Computational simulations, including molecular dynamics using LAMMPS with the General AMBER Force Field and density functional theory calculations, were performed to investigate CO_2 absorption behavior. The simulation system consisted of 140 citric acid molecules, 200 N-methylmorpholine molecules, and 40 CO_2 molecules. Structural, transport, and reactivity properties were analyzed using radial distribution functions (RDF), mean square displacement (MSD), and quantum chemical descriptors. RDF analysis revealed pronounced intermolecular interactions between CO_2 molecules and the functional groups of the DES components, indicating preferential structuring around the solvent molecules. The diffusion coefficient calculated from the MSD analysis was 4.879×10^{-12} m^2 s^{-1}, suggesting moderate mobility of CO_2 molecules within the solvent environment.

Paper type: Research Paper

Keywords: Deep eutectic solvent, Capture of CO_2, DFT, Molecular modeling, Computational simulation.

Citation: Al-Mahameed, B. K. M., "CO_2 Capture Using a Citric Acid and N-Methylmorpholine Deep Eutectic Solvent: A Computational Study," *Jordanian Journal of Engineering and Chemical Industries*, Vol. 9, No. 1, pp: 44–62 (2026).

* Corresponding author: E-mail: BaraaAlmahameed@bau.edu.jo ORCID: 0009-0002-4300-3327

Received: 19/January/2026 Revised: 08/March/2026

Jordanian Journal of Engineering and Chemical Industries (JJECI), Vol.9, No.1, 2026, pp: 44-62 Accepted: 10/March/2026

1. Introduction

Carbon dioxide is one of the main greenhouse gases, and the rapid increase in atmospheric levels has led researchers to adopt practical and sustainable strategies to reduce these dangerous emissions (Filonchyk et al., 2024; Zhang et al., 2024). Many methods have emerged to reduce these emissions, and methods for absorbing carbon dioxide gas using deep eutectic solvents (DESs) have gained wide attention for their high absorption capacity, flexibility across different operating conditions, and selectivity (Geweda et al., 2025).

These solvents are prepared by forming a hydrogen bond between two substances, one a hydrogen donor and the other an acceptor, at specific temperatures and pressures. This process results in a mixture with a melting point much lower than the individual melting points of the two components (Smith et al., 2014). DESs possess a range of advantages that have made them the focus of widespread interest, as they are easy to prepare and low in cost due to the abundance of their components, and they exhibit chemical and thermal stability, as well as high extraction and reactive performance. They are also identified by their wide ability to dissolve various materials, as well as their recoverability and recyclability (Luo et al., 2021).

Given the flexibility in preparing of these solvents, they can be designed specifically for certain tasks-such as gas absorption, improving solubility, or modified kinetic properties - thereby enhancing their various applications (Elhamarnah et al., 2024). Recent studies have demonstrated that DESs composed of various combinations of organic acids, amines, and quaternary ammonium salts exhibit strong interactions with CO_2, confirming their potential for efficient gas capture (Pelaquim et al., 2021).

Theoretical and experimental studies on CO_2 capture using deep eutectic solvents (DESs) have provided insights into both the functional performance and the molecular mechanisms involved. Early experimental research on choline chloride-based DESs, such as ethaline (ChCl:ethylene glycol) and reline (ChCl:urea), showed that solvent polarity and hydrogen bonding networks were responsible for the physical absorption of CO_2 and the solubility of CO_2 (Ali et al., 2014; Leron et al., 2013; Leron & Li, 2013). Later research investigated task-specific amine-functionalized DESs, which achieved greater absorption capabilities and selectivity by chemically forming carbamate and bicarbonate in addition to physically absorbing CO_2 (Hack et al., 2022; Ismail et al., 2024).

Recent experiments (Abdrabou et al., 2023; Cichowska-Kopczyńska et al., 2023; Coin et al., 2025) have focused on reducing viscosity, enhancing diffusivity, and optimizing Hydrogen bond donor (HBD) / Hydrogen bond acceptor (HBA) combinations to increase CO_2 solubility under moderate conditions. Simultaneously, computational studies have played a crucial role in understanding absorption mechanisms and optimizing solvent formulations. Density Functional Theory(DFT) and Molecular Dynamics (MD) simulations have identified preferred CO_2 interaction sites in DES matrices, quantified hydrogen bonding and free volume effects, and predicted diffusivity trends based on experimental measurements(Chi et al., 2025; Ismael et al., 2009; Ma et al., 2021).

In recent years (2023-2025), hybrid techniques integrating the COnductor-like Screening MOdel for Real Solvents (COSMO-RS), Ab initio molecular dynamics (AIMD), and machine learning have evolved to estimate CO_2 solubility, evaluate thermodynamic feasibility, and aid in rational design of high-performance DESs (Lemaoui et al., 2023; Mohan et al., 2023; Mohan et al., 2024). Theoretical and experimental studies show that functionalized and amino acid-based DESs provide varied, customizable, and durable CO_2 capture methods, bridging fundamental understanding and potential industrial uses.

Most recent studies on DESs for CO_2 capture have mainly emphasized choline chloride–based systems, due to their proven effectiveness. Much less attention has been given to alternative, bio-derived solvents that could offer advantages such as renewability and reduced environmental impact. In this study, citric acid and N-methylmorpholine (NMM) were selected as components of a deep eutectic solvent based on their complementary hydrogen-bonding roles. Citric acid, which contains three carboxyl (–COOH) groups and one hydroxyl (–OH) group, acts primarily as a hydrogen bond donor (HBD)(Abbott et al., 2003). In contrast, NMM, a tertiary amine lacking N–H bonds, functions as a hydrogen bond acceptor (HBA) through the lone pairs on its nitrogen and ether oxygen atoms(Desiraju & Steiner, 2001).

The interaction between the proton-donating acidic groups of citric acid and the electron-rich acceptor sites of NMM is expected to promote strong intermolecular hydrogen bonding. Such interactions may induce significant melting point depression, thereby facilitating the formation of a stable deep eutectic solvent(Abbott et al., 2013). Moreover, the basic nitrogen center and polar oxygen functionality in NMM, together with the acidic and polar groups of citric acid, may provide favorable interaction sites for CO_2 through acid–base interactions and non-covalent forces. Given the well-established efficiency of amine-based systems in CO_2 absorption, the citric acid/NMM DES is therefore expected to exhibit strong potential for carbon dioxide capture. However, this system has not been extensively investigated, motivating its evaluation using DFT and MD simulations.

2. Computational Methods

2.1 Softwares

ORCA 5.0, Avogadro, Multiwfn,VMD (visual molecular dynamic), Packmol, and Lammps

2.2 Quantum Chemical Calculations

2.2.1 Geometry optimization

This study used the DES system, which contains N-methylmorpholine (as HBA) and citric acid (as HBD). These compounds were studied as separate molecules to achieve optimum energy minimization. This protocol was implemented using the ORCA 5.0 program (Neese, 2025) . The geometry optimization was carried out using DFT with B3LYP functional and 6-311 G (d,p) basis set. The results from ORCA were displayed using Avogadro(Hanwell et al., 2012), Multiwfn (Lu & Chen, 2012) and VMD (Humphrey et al., 1996) programs. **Figures 1** and **Figure 2** show the optimized structures of citric acid and N-methylmorpholine, respectively. The citric acid/N-methylmorpholine cell was constructed by using Avogadro program. A cubic simulation box of 80×80×80 $Å^3$ was constructed, containing 140 molecules of citric acid and 200 molecules of NMM, as shown in **Figure 3**, with periodic boundary conditions applied in all directions. The initial packing process involved 1000 tries and a minimum intermolecular spacing of 5×10^{-5} Å. The optimization of cell was performed by using ORCA 5.0 and Packmol (Martínez et al., 2009)program under NPT ensemble at 298 k and 1 atm for 200 ps to minimize energy and equilibrate the system.

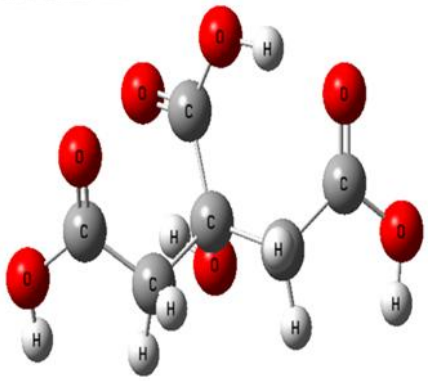

Fig 1. Geometry-optimized of citric acid

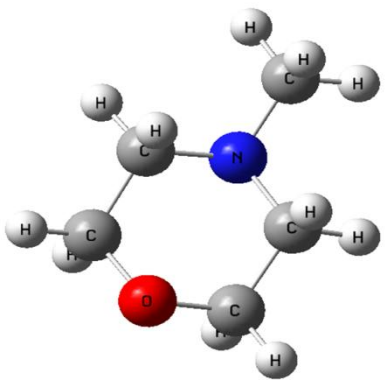

Fig 2. Geometry-optimized of NMM

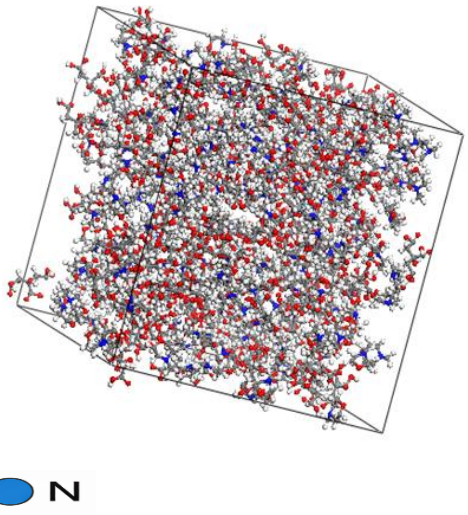

Fig 3. Constructed cell of the citric acid–NMM system

2.2.2 Frontier Molecular Orbitals Analysis Method (FMOs)

The lowest unoccupied molecular orbital (LUMO) and the highest occupied molecular orbital (HOMO) are the main orbitals used to assess compound stability and reactivity. A low E_{LUMO} value indicates that the molecule readily accepts electrons. A high E_{HOMO} value shows the compound readily donates an electron to a receptor molecule. The difference between HOMO and LUMO energies is called the energy gap (ΔE)(Fleming, 2011; Parr, 1989).

Quantum chemical computations were performed using ORCA 5.0. The molecular geometry was optimized at ground-state structures using DFT with the B3LYP functional and the 6-311 G (d, p), which is a triple-zeta valence basis set with polarization functions. This step enabled evaluation of reactivity characteristics. The following equations, which relate the HOMO and LUMO energies to the ionization potential and electron affinity, were used to calculate the molecular indices (Rocha et al., 2015; Zhan et al., 2003). The result of FMOs analysis was shown in Figure 4.

$$\text{Energy gap } (E_{Gap}) = E_{LUMO} - E_{HOMO} \quad (1)$$

$$\text{Ionization potential } (I) = -E_{HOMO} \quad (2)$$

$$\text{Electron affinity } (A) = -E_{LUMO} \quad (3)$$

$$\text{Chemical hardness } (\eta) = \frac{(I - A)}{2} \quad (4)$$

$$\text{Chemical potential } (\mu) = \frac{-(I + A)}{2} \quad (5)$$

$$\text{Softness } (\sigma) = \frac{1}{\eta} \quad (6)$$

$$\text{Electronegativity } (\chi) = \frac{-(E_{HOMO} + E_{LUMO})}{2} \quad (7)$$

$$\text{Electrophilicity } (\omega) = \frac{\mu^2}{2\eta} \tag{8}$$

2.2.3 Molecular Electrostatic Potential (MEP)

The molecular electrostatic potential explains the distribution of charges, the sites of electrophilic and nucleophilic assaults inside the molecule, and molecular reactivity (Gadre et al., 2021; Suresh, 2022). The colored map shown may be constructed by using specific forces acting on various species in the molecule, resulting in projected potential based on the electron cloud and nuclei at a given position. MEP is stated as the following equation:

$$V(r) = \sum_{A}^{N} \frac{Z_A}{r - R_A} - \rho(r')\, d^3r'(r - r') \tag{9}$$

In this study, MEP analysis was performed using ORCA 5.0. The result was displayed in the Multiwfn program; the MEP 3D colored map of citric acid, NMM, and DES was shown in Figure 5, demonstrating a considerable increase in potential pass through from the red color scale (more negative value) to the blue color scale (more positive value). Red signifies the biggest negative electrostatic potential area, whereas blue denotes a positive electrostatic potential (Gadre et al., 2021; Suresh, 2022).

2.2.4 Reduced Density Gradient (RDG)

The reduced density gradient (RDG) analysis was used to identify noncovalent bond interactions (NCIs) between distinct parts of the molecule; it is based on the electron density $\rho(r)$ and its gradient $\nabla\rho(r)$ (Johnson et al., 2010), the formula is

$$RDG = \frac{1}{2(3\pi^2)^{(\frac{1}{3})}} \frac{|\nabla\rho(r)|}{\rho(r)^{(\frac{4}{3})}} \tag{10}$$

In general, the various noncovalent interactions are denoted by different color codes, where the blue hue signifies a strong hydrogen bonding (HB) attraction, electrostatic attraction such as VDW (green color scale), and steric hindrance (red color scale), which is described as being attributed to the optimized molecular orientation on the surface leading to intense close contacts and this point exports the stability of the absorption system. The unfavorable red spike is observed in all the analyzed systems, indicating the possibility of instability. However, this repulsion type is formed by the molecule itself depending on the amount of cyclic rings, whereas the surface of contact generated a green attracting layer in most cases (Contreras-García et al., 2011; Johnson et al., 2010). The RDG analysis was performed using ORCA 5.0, the results were displayed using Multiwfn program, as shown in Figure 6.

2.2 Molecular Dynamic simulation

2.3.1 CO2-DES system

Forty molecules of optimized carbon dioxide were added into the constructed cell of the citric acid–NMM system, as shown in Figure 7. The geometry optimization of the cell was performed using ORCA and Packmol program under the same conditions as the previously created solvent cell. After optimization, a molecular dynamics simulation was performed. The simulations investigated the structural and dynamical properties of the CO_2–DES system.

2.3.2 Simulation parameters

Molecular dynamics (MD) simulations were carried out using the LAMMPS simulation package at 298 K. The intermolecular interactions were described using the General AMBER Force Field (GAFF2). Lennard–Jones interactions were modeled with a cutoff distance of 12 Å, while long-range electrostatic interactions were treated using the particle–particle particle–mesh (PPPM) method with an accuracy of 1×10^{-4}. Atomic partial charges were assigned using the AM1-BCC scheme through AmberTools, incorporated into the topology, and kept fixed during the simulations. Lorentz–Berthelot mixing rules and AMBER scaling factors for bonded interactions (special_bonds amber) were applied. The simulation system consisted of 140 citric acid molecules, 200 N-methylmorpholine (NMM) molecules, and 40 CO_2 molecules, resulting in a total of 6660 atoms. The initial configuration of the system was generated using Packmol in a cubic simulation box of 80 × 80 × 80 Å under periodic boundary conditions (PBC) applied in the x, y, and z directions. Energy minimization was first performed using the conjugate gradient algorithm. The system was equilibrated in the NPT ensemble at 298 K and 1 atm for 1 ns using a timestep of 1 fs. During this stage, the simulation box relaxed to an equilibrated size of 41.34 × 41.34 × 41.34 Å, corresponding to an average density of 1.149 g cm^{-3}, indicating that the system reached a stable liquid-phase structure prior to the production stage. After equilibration, a 2 ns production simulation was carried out in the NVT ensemble with a timestep of 1 fs. The diffusion coefficient of CO_2 was calculated from the slope of the mean square displacement (MSD) in the linear diffusive regime. The detailed molecular dynamics simulation parameters are summarized in **Table 1**.

Table 1. Simulation parameters

Simulation parameters	
Software	
MD program	LAMMPS
Initial configuration	Packmol
Topology & charges	GAFF2 via Amber Tools (AM1-BCC)
Molecules	140 Citric acid + 200 NMM + 40 CO_2
Total atoms	6660
Initial Box size (Packmol)	80 × 80 × 80 Å (PBC in x,y,z)
Equilibrated box size (after NPT)	41.34 × 41.34 × 41.34 Å
Functional form	GAFF2 (bonded + Lennard-Jones + Coulomb)
Cutoff	12.0 Å
Long-range electrostatics	Particle-Particle-Particle-Mesh (PPPM) (accuracy 1×10^{-4})
Mixing rule	Lorentz–Berthelot
1–4 scaling	special_bonds amber
Units	Real
Atom style	Full
Thermostat	Nose-Hoover
Barostat	Nose-Hoover
Minimization	Conjugate gradient (2000–20000 steps)

Equilibration	NPT, 298 K, 1 atm, 1000000 steps,1 fs, 1 ns
Production	NVT, 298 K, 2000000 steps, 1.0 fs, 2 ns
Diffusion	MSD (fit after ballistic regime, 1 ns)

2.3.3 Trajectory Analysis Methods

2.3.3.1 Radial Distribution Function (RDF)

The Radial Distribution Function (RDF) is a fundamental tool for studying the spatial distribution of particles around a reference molecule, enabling characterization of the molecular system's spatial structure. This function describes the arrangement patterns and relative distribution of molecules, and reflects the nature of their interactions (Ortega et al., 1997). In this, the RDF analysis was performed between selected atom pairs. The interaction between the carbon atom in CO2 and the nitrogen atom of NMM (C_CO_2 - N_NMM) was investigated in order to investigate potential Lewis acid-base effects. To assess possible hydrogen bonding, the interaction between the hydrogen atoms in the DES and the CO_2 oxygen atom was also examined.

The RDF analyses were computed using LAMMPS at 298 K under NVT Conditions. The results are presented in Section 3.6.1, in **Figure 9.**

2.3.3.2 Mean square displacement (MSD)

The average displacement of particles over time is described by Mean Square Displacement (MSD), a crucial metric in molecular dynamics. It sheds light on how molecules move through a system and how they diffuse(Allen & Tildesley, 2017). The definition of MSD is:

$$MSD(t) = (|r(t) - r(0)|)^2 \quad (11)$$

The Einstein relation for the 3D system can be used to estimate the diffusion coefficient D using MSD, where r(t) is the position of a particle at time t and r(0) is the average over all particles and time origins.

$$D = \frac{1}{2n}\frac{d}{dt}MSD(t) \quad (12)$$

The MSD analysis was computed in LAMMPS after initial ballistic region at 298 K under NVT Conditions. The results are presented in Section 3.6.2, in Figure 10.

The plots in MD section were generated using Python (Matplotlib) from LAMMPS output data.

3. Results and Discussion

3.1 Optimized Structures

The optimized structure of citric acid is shown in **Figure 1**, while the optimized NMM molecule is presented in **Figure 2**. The constructed simulation cell containing 140 citric acid and 200 NMM molecules is illustrated in **Figure 3**.

3.2 Frontier Molecular Orbitals (FMOs)

FMO analysis was used to investigate the electronic behavior of citric acid, N-methylmorpholine (NMM), and designed deep solvents. For NMM, the HOMO is distributed around nitrogen and oxygen atoms, and the LUMO is distributed over C-O and C-N bonds. In citric acid the HOMO is mainly around oxygen atoms in the carboxyl and hydroxyl groups, while the LUMO is concentrated around the carbon atoms in the carbonyl groups. Therefore, hydrogen bonding is mainly formed between citric acid and NMM, where the hydrogen atom of the carboxyl group in citric acid interacts with the electron-rich oxygen or nitrogen atom in NMM. This interaction occurs between the electron-donating HOMO region of citric acid and the electron-accepting LUMO region of NMM, facilitating hydrogen bond formation. The HOMO region represents areas of high electron density capable of donating electrons, whereas the LUMO region represents sites that can accept electron density, which promotes intermolecular interactions and contributes to the decrease in melting point and the stability of the DES structure. The solvent contains several sites that enhance carbon dioxide absorption. The nitrogen atom in NMM has a lone electron pair that can react with carbon dioxide through a Lewis acid-base interaction. The oxygen atoms in the carbonyl and hydroxyl groups of citric acid, with their non-bonding electrons, can also interact with carbon dioxide through van der Waals forces or weak hydrogen bonds. Additionally, hydrogen atoms bonded to oxygen in OH^- or COOH groups may form weak hydrogen bonds with carbon dioxide. Together, these sites support efficient carbon dioxide capture. The FMO energy levels of citric acid, NMM, and (citric acid +NMM) DES system is shown in **Figure 4**.

The reduction in the HOMO–LUMO gap compared to the individual components suggests enhanced reactivity and improved affinity of the DES for CO_2 capture, as shown in **Table 2**.

According to **Table 2**, the reactivity descriptors were evaluated based on orbital energy. The DES exhibits low chemical hardness and high softness. This indicates enhanced chemical reactivity. The chemical potential and electronegativity of DES differ from those of its individual components, indicating electronic redistribution within the DES. The electrophilicity increased, indicating the ability to accept electrons. The DES exhibits higher affinity toward CO_2 compared to its individual components (citric acid and NMM), indicating enhanced capture performance.

Table 2. Quantum chemical reactivity parameters of compounds

	E_{GAP}	I	A	η	μ	X	ω	σ
Citric acid	0.178172	0.240247	0.062075	0.089086	-0.15116	0.15116	0.128245	5.612554
NMM	0.232252	0.182336	-0.049916	0.116126	-0.06621	0.06621	0.018875	4.305668
DES	0.096805	0.19128	0.094475	0.048403	-0.14288	-0.14288	0.210877	10.33004

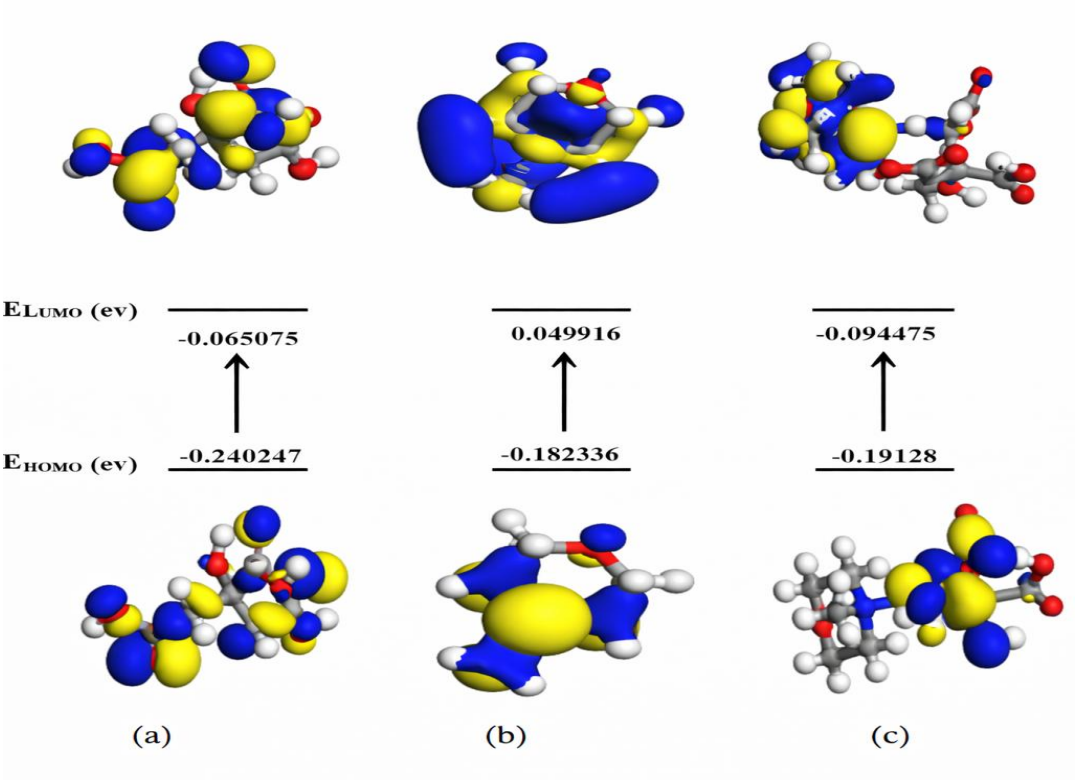

Fig 4. Energy levels of FMOs for (a) citric acid (b) NMM and (C) DES

3.3 Molecular Electrostatic Potential (MEP)

In NMM, the red color is concentrated around the oxygen atom, indicating that this region has a negative electrostatic potential. The remaining atoms that make up NMM are almost light green, indicating they are neutral. In citric acid, the blue color is distributed around the hydrogen atom that bonds to the hydroxyl group, indicating a positive electrostatic potential. The remaining atoms that make up citric acid are almost light green, meaning they are neutral. These results support the formation of a hydrogen bond between the hydrogen atom in citric acid and the oxygen atom in NMM, as shown in **Figure 5**.

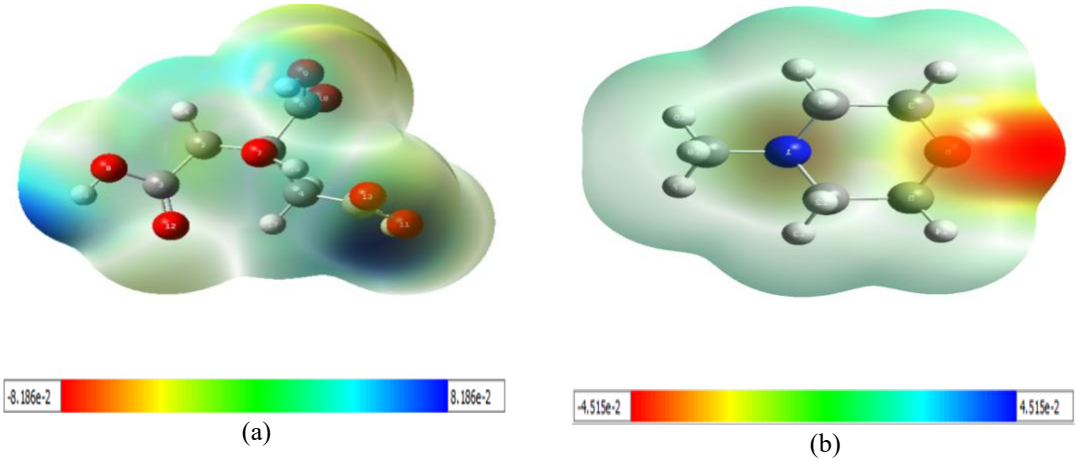

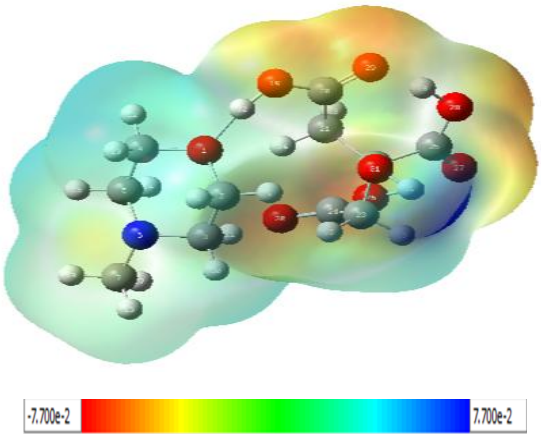

(c)

Fig 5. 3D-MEP surface of (a) Citric acid, (b) N-Methylmorpholine, and (c) DES (Red and yellow color scales refer to electron-rich sites, pale and dark blue color scales refer to electron-poor sites)

3.4 Reduced Density Gradient (RDG)

For citric acid alone, strong intramolecular hydrogen bonds are evident between the hydroxyl and carboxyl groups, as indicated by the pronounced blue regions in the RDG isosurfaces and negative peaks in the sign(λ_2)ρ plot. A noticeable repulsion was also observed, resulting from the proximity of oxygen-rich functional groups, which led to the prominence of red areas on the isosurface. In contrast, the NMM behavior is limited to weak non-covalent interactions, dominated by van der Waals forces, with a limited contribution from hydrogen bonds. The RDG plots show mostly green surfaces with minor steric contributions, suggesting relatively weak intermolecular stabilization. Upon formation of the DES (citric acid + NMM), a significant shift in the interaction profile is observed. Strong intermolecular hydrogen bonds form, clearly represented by blue regions and sharp negative peaks in the sign(λ_2)ρ function. Simultaneously, the internal hydrogen bonding within citric acid decreases, as these groups become engaged in intermolecular interactions with NMM. More van der Waals interactions (green areas) appear, which help solidify the supramolecular network. Overall, the comparison shows that citric acid and NMM have limited or localized noncovalent interactions when they are alone, but when combined together to form a DES, they produce a framework of interactions that is dominated by strong hydrogen bonds and supported by van der Waals forces, which makes the structure more stable, as shown in **Figure 6**.

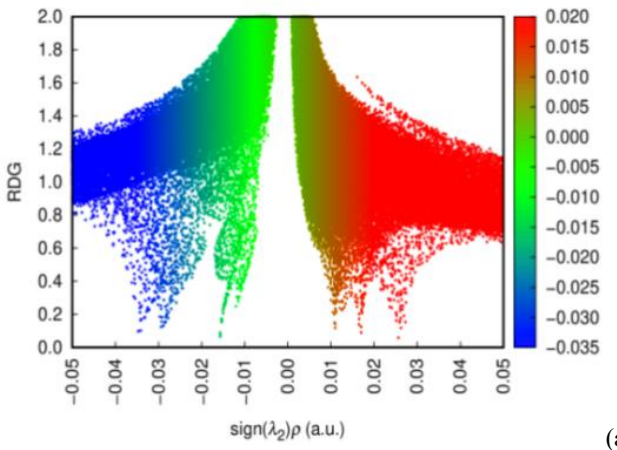

(a)

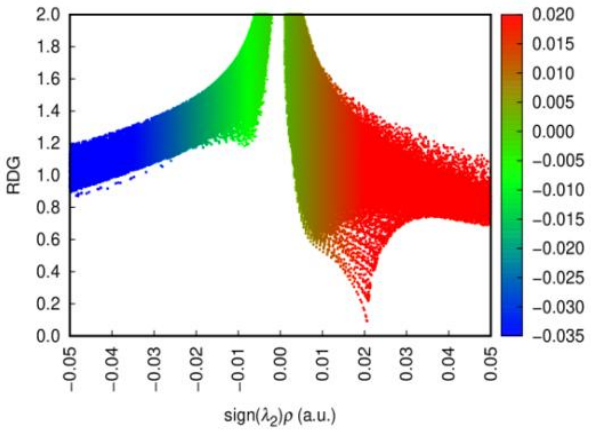

(b)

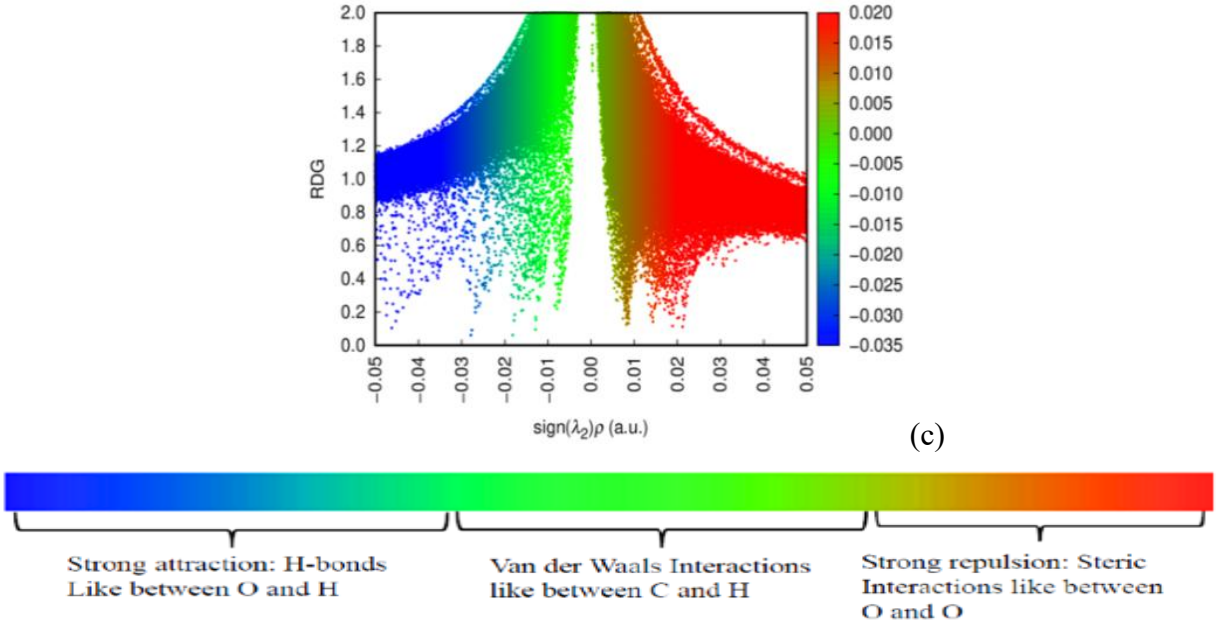

Fig 6. RDG for (a) Citric acid, (b) NMM and (c) DES.

3.5 CO_2–DES Interactions

A simulation cell containing 140 citric acid, 200 NMM, and 40 CO_2 molecules was constructed and subsequently optimized, as shown in **Figure 7.**

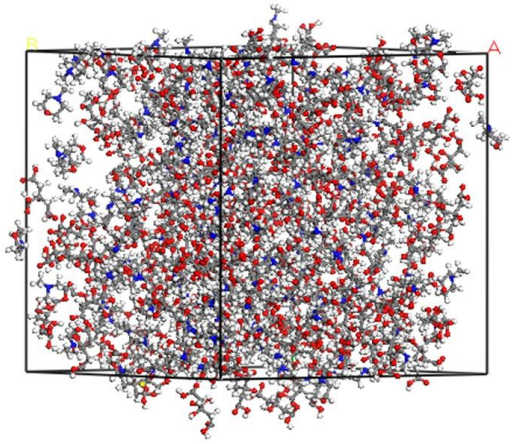

Fig 7. Constructed cell of citric acid-NMM-CO_2

3.6 Molecular Dynamics Results

The dynamic simulation of DES during CO_2 capture appears highly stable thermodynamically. The total energy was estimated to be 8750 Kcal/mol. The energy–time profile exhibits small fluctuations around an average value, indicating that the system is stable. The temperature during the dynamic simulation, which is mostly constant, is approximately 298 K with small fluctuations between nearly

292 and 310 K. Both the temperature and energy profiles, as shown in **Figure 8**, indicate that the system has reached thermal equilibrium under the conditions listed in Table 1.

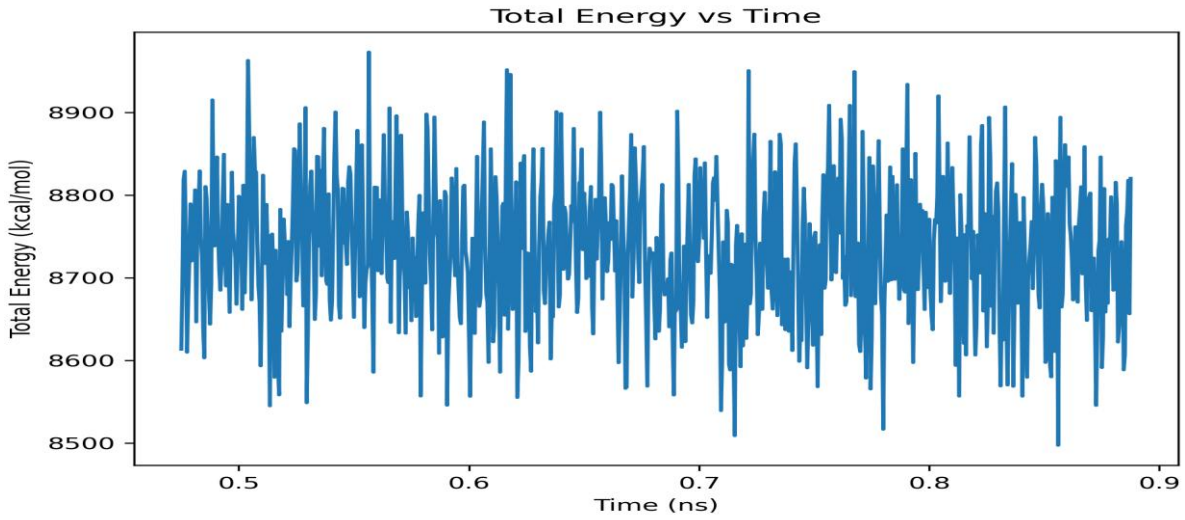

(a)

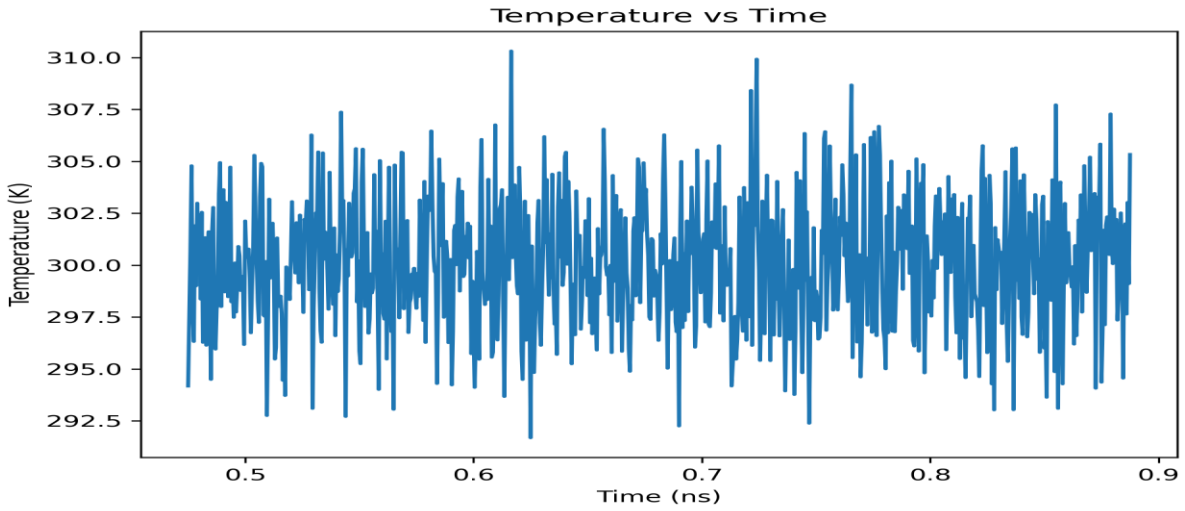

(b)

Fig 8. Molecular Dynamics Simulations of CO_2 Capture by Deep Eutectic Solvents (a) Energy vs time (b) Temperature vs time.

3.6.1 Radial Distribution Function (RDF)

Analysis of the radial distribution functions **Figure 9**, with the corresponding structural parameters summarized in Table 3, reveals a pronounced first peak for the CO_2–citric acid (O···H in OH) pair at 1.78 Å with g(r) = 3.93, indicating strong short-range interaction between CO_2 and the hydroxyl groups of citric acid. In contrast, the CO_2–N-methylmorpholine correlation appears only as a weak and broad feature at 5.88 Å (g(r) = 1.35), suggesting limited structural contribution.

A comparison between the O_CO_2–H2 and O_CO_2–H5 pairs further confirms that the interaction involving the hydroxyl hydrogen (O–H···O) is significantly stronger than that involving hydrogen atoms bonded to carbon (C–H···O). The O_CO_2–H5 pair exhibits a weak and broad peak at 3.98 Å with g(r) = 0.79, indicating negligible hydrogen bonding between CO_2 and the C–H sites of citric acid. This behavior is consistent with the well-established weakness of C–H···O interactions compared to conventional O–H···O hydrogen bonds. These findings indicate that CO_2 preferentially associates with the hydroxyl groups of citric acid within the DES network rather than being uniformly distributed throughout the solvent. This preferential interaction promotes local structuring of CO_2 molecules around the hydroxyl sites of the solvent components.

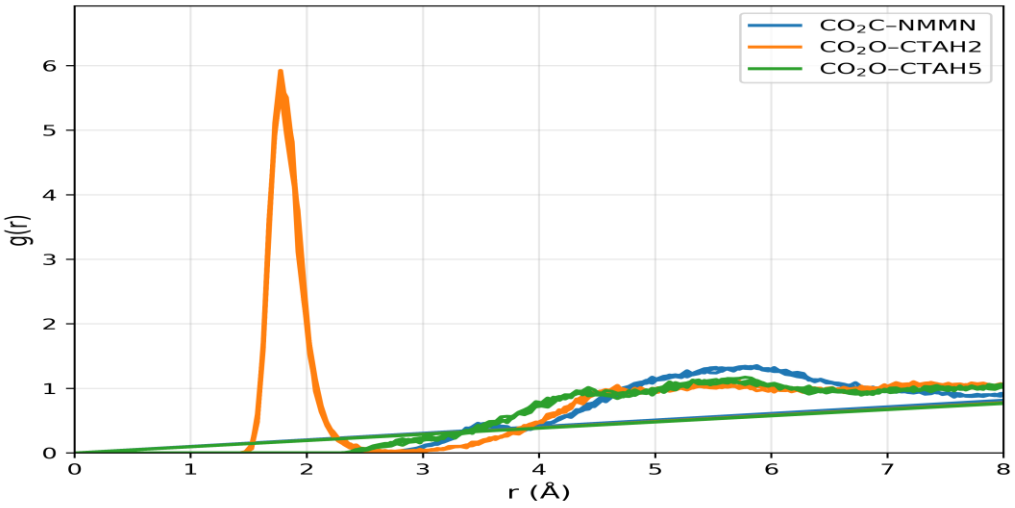

Fig 9. Radial distribution function for the citric acid–NMM–CO_2 system.

*H2→ represents hydrogen bonded to oxygen in (OH) group
*H5→ represents hydrogen bonded to carbon
*CTA→ citric acid

Table 3. Radial distribution function for DES–CO_2 system.

Interaction	r (A^o)	g(r)	Interpretation
CO_2-NMM (C-N)	5.88	1.35	Weak, long-rang correlation
CO_2-Citric acid (O - (H in OH)	1.78	3.93	Strong short-range association indicating CO_2 confinement near OH groups
CO_2-Citric acid (O- (H in C-H)	3.98	0.79	Negligible interaction

3.6.2 Mean Square Displacement (MSD)

The diffusion coefficient of CO_2 in the deep eutectic solvent (DES) was determined from molecular dynamics simulations using the slope of the mean square displacement (MSD) curve, as shown in **Figure10**. The calculated value, D = 4.879×10^{-12} m^2/s,

is significantly lower than that of CO_2 in water at 25 °C (1.95×10^{-9} m²/s (Allen & Tildesley, 2017), and also lower than the reported experimental values for CO_2 in DESs at infinite dilution (1.44×10^{-11}–2.90×10^{-10} m²/s) (Xin & van Sint Annaland, 2023), as shown in Table 4. The MSD curve exhibits a well-defined linear regime at long simulation times, confirming diffusive behavior and convergence of the slope. The diffusion coefficient was therefore extracted by linear fitting over the last 1 ns of the trajectory, minimizing contributions from the initial non-diffusive regime. The lower diffusion coefficient observed in the simulation can be attributed to the fact that the molecular dynamics model represents a concentrated periodic DES system with a fixed CA:NMM molar ratio, rather than the infinite dilution conditions typically used in experimental measurements. In such concentrated DES systems, strong intermolecular interactions and the relatively high viscosity of the hydrogen-bonded solvent network significantly restrict the mobility of dissolved CO_2 molecules. This behavior is consistent with the RDF analysis, which revealed strong and localized interactions between CO_2 molecules and the hydroxyl groups of citric acid within the DES structure. These localized interactions within the hydrogen-bond network limit long-range molecular motion and consequently reduce the diffusion coefficient. Although slower diffusion implies reduced mass transport, it also reflects stronger gas–solvent interactions and enhanced CO_2 retention within the DES, which may be advantageous for carbon capture applications.

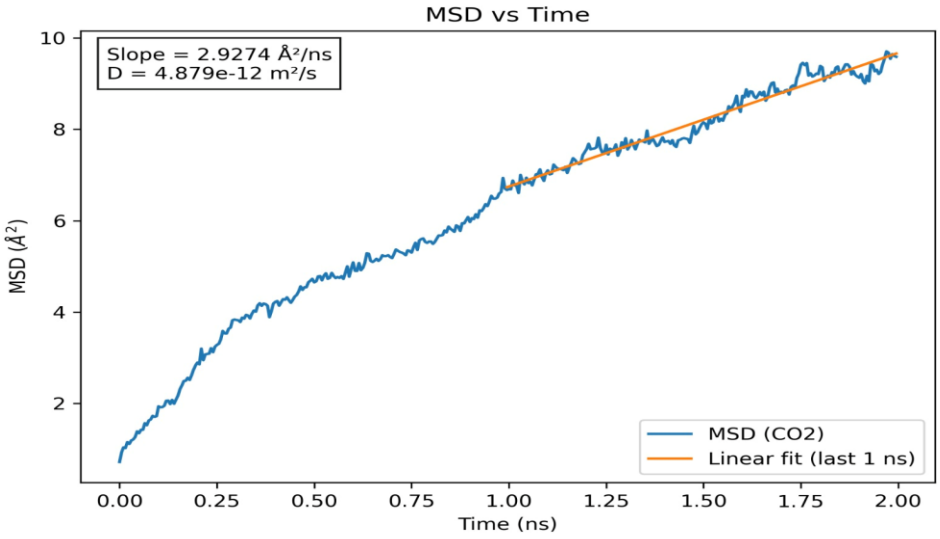

Fig 10. MSD versus simulation time for the citric acid–NMM–CO_2 system.

Table 4. Comparison of CO_2 Capture Performance of DES Systems

DES System (HBA:HBD)	Ratio (HBA:HBA)	Co-solvent	Ratio (DES:Solvent)	Method	T (K)	D_{CO2} (m^2/sec)	Reference
Citric acid : NMM	1:1.43	-	-	MD	298	4.9×10^{-12}	This work
ChCl : Urea	1:2	-	-	MD	298	2.0×10^{-11}	(Dawass et al., 2022)
		Methanol	3:2			4.2×10^{-10}	
ChCl : EG	1:2	-	-	MD	298	9.0×10^{-11}	(Dawass et al., 2022)
		Propylene carbonate	3:2			3.7×10^{-10}	

		Methanol	3:2			6.1×10^{-10}	
Ch:MEA	1:6	-	-	MD	298	1.6×10^{-10}	(Zhang et al., 2021)
		water	H_2O 98%			1.08×10^{-9}	
TBPBr:TEG	1:1	-	-	MD	298	4.17×10^{-10}	(Nandi et al., 2025)
ChCl:GLY	1:2	-	-	Experimental	298	1.9×10^{-11}	(Xin & van Sint Annaland, 2023)
ChCl:FA	1:4	-	-	Experimental	298	3.4×10^{-10}	

3.7 Industrial Feasibility and Safety Considerations

Beyond the molecular-level insights presented in this work, safety and industrial applicability must also be considered when evaluating the citric acid/NMM deep eutectic solvent for CO_2 capture. Although DESs are often described as green solvents, their environmental and safety profiles depend on the properties and interactions of their individual components, and toxicity should not be assumed negligible without proper evaluation(Hayyan et al., 2013; Paiva et al., 2014). Citric acid used in this work as a hydrogen bond donor is a biodegradable acid composed of three carboxyl groups and one hydroxyl group. It has been widely used in the food and pharmaceutical industries and is recognized as a safe substance. However, due to its acidic nature (pKa ≈3.1), some degree of corrosion under industrial conditions cannot be ruled out. Nevertheless, within the deep eutectic solvent structure, the hydrogen bonding network formed with the hydrogen bond acceptor is expected to modify proton availability, thus reducing the effective acidity compared to the pure acid (Apelblat, 2014; Książek, 2024).N-methylmorpholine is a flammable tertiary amine with moderate acute toxicity and a boiling point of approximately 116 °C. In this work, it was used as a hydrogen bond acceptor. When combined with citric acid to form a deep eutectic solvent, it is expected to exhibit reduced volatility compared to the free amine consistent with the generally low vapor pressures reported for DES systems. Since the regeneration temperatures in amine-based CO_2 capture processes are typically between 90 and 120 °C, significant volatility is not expected under controlled operating conditions(National Center for Biotechnology, 2026; Smith et al., 2014).Nevertheless, a comprehensive assessment of long-term thermal stability and corrosion behavior would require dedicated experimental investigations, such as thermogravimetric analysis coupled with evolved gas analysis to monitor potential volatile emissions, as well as electrochemical corrosion measurements under process-relevant conditions. These evaluations are beyond the scope of the present computational study. While the current findings demonstrate favorable molecular-level performance, further experimental validation is necessary prior to large-scale industrial application.

4. Conclusions

In this study, a deep eutectic solvent (DES) composed of citric acid and N-methylmorpholine (NMM) was investigated for CO_2 capture using molecular dynamics simulations and density functional theory (DFT) calculations. Frontier molecular orbital (FMO) analysis revealed the possibility of hydrogen bond formation between the solvent components. The interaction occurs between the electron-rich oxygen atom of citric acid, corresponding to the HOMO region, and the electron-deficient region of N-methylmorpholine associated with the LUMO, facilitating intermolecular hydrogen bonding within the DES structure. The presence and probability of hydrogen bonding were further supported by molecular electrostatic potential (MEP) analysis, which indicated favorable electrostatic interactions between the oxygen atom of citric acid and the hydrogen atom involved in hydrogen bonding. These results are consistent with the structural analysis of the system. This is further supported by the RDF analysis, indicating strong short-range interactions between CO_2 molecules

and the hydroxyl groups of citric acid. In addition, the diffusion coefficient obtained from the mean square displacement (MSD) analysis suggests that CO_2 molecules exhibit reasonable mobility within the solvent environment. Overall, the computational results provide theoretical evidence that the investigated deep eutectic solvent possesses promising characteristics as a potential solvent for CO_2 capture applications. Future work should investigate the effects of temperature, pressure, water content, viscosity, CO_2 solubility, and the presence of other gases on the absorption performance, as well as conduct experimental studies to validate the computational predictions.

CRediT Author Contribution Statement

Baraa K. Al-Mahameed: Conceptualization, Methodology, Software, Formal Analysis, Investigation, Visualization, Writing – Original Draft, Writing – Review & Editing.

Declaration Statements

Funding

This research received no external funding.

Conflicts of Interest

The authors declare no conflict of interest.

Use of AI Tools (if applicable)

During the preparation of this work, the author used AI tools to do paraphrasing.

Nomenclature

Symbol	Description	Unit
ΔE	Energy gap	eV
I	Ionization potential	eV
A	Electron affinity	eV
H	Chemical hardness	eV
μ	Chemical potential	eV
σ	Chemical Softness	1/eV
X	Electronegativity	eV
ω	Electrophilicity	eV
BE	Binding energy	kcal/mol
RDF	Radial Distribution Function	Å
MSD	Mean Square Displacement	$Å^2$
MEP	Molecular Electrostatic Potential	V

Symbol	Description	Unit
LUMO	Lowest Unoccupied Molecular Orbital	eV
HOMO	Highest Occupied Molecular Orbital	eV
CO_2	Carbon Dioxide	-
D	Diffusion coefficient	m^2/sec
DES	Deep eutectic solvent	-
HBA	Hydrogen Bond Acceptor	-
HBD	Hydrogen Bond Donor	-
NMM	N-methylmorpholine	-
FMOs	Frontier Molecular Orbitals	-
RDG	Reduced Density Gradient	-
DFT	Density Functional Theory	-
MD	Molecular Dynamics	-
ChCl	Choline Chloride	-
TEG	Triethylene Glycol	-
FA	Furfuryl Alcohol	-
MEG	Monoethylene Glycol	-
TBPBr	Tetrabutylphosphonium Bromide	-
EG	Ethylene Glycol	-

References

Abbott, A., Azam, M., Ryder, K. S., & Saleem, S. (2013). *Anal. Chem.*, *85*, 6653.

Abbott, A. P., Capper, G., Davies, D. L., Rasheed, R. K., & Tambyrajah, V. (2003). Novel solvent properties of choline chloride/urea mixtures. *Chemical communications*(1), 70-71.

Abdrabou, H. K., AlNashef, I., Abu Zahra, M., Mokraoui, S., Ali, E., & Hadj-Kali, M. K. (2023). Experimental investigation of novel ternary amine-based deep eutectic solvents for CO2 capture. *PLoS One*, *18*(6), e0286960. https://doi.org/10.1371/journal.pone.0286960

Ali, E., Hadj-Kali, M. K., Mulyono, S., Alnashef, I., Fakeeha, A., Mjalli, F., & Hayyan, A. (2014). Solubility of CO2 in deep eutectic solvents: Experiments and modelling using the Peng–Robinson equation of state. *Chemical Engineering Research and Design*, *92*(10), 1898-1906. https://doi.org/https://doi.org/10.1016/j.cherd.2014.02.004

Allen, M. P., & Tildesley, D. J. (2017). *Computer simulation of liquids*. Oxford university press.

Apelblat, A. (2014). *Citric acid*. Springer.

Chi, H. Y., Tsao, H. K., & Sheng, Y. J. (2025). Mechanisms of CO(2) Absorption in Amino Acid-Based Deep Eutectic Solvents: Insights from Molecular Dynamics and DFT Calculations. *J Phys Chem B*, *129*(23), 5779-5787. https://doi.org/10.1021/acs.jpcb.5c00558

Cichowska-Kopczyńska, I., Nowosielski, B., & Warmińska, D. (2023). Deep Eutectic Solvents: Properties and Applications in CO(2) Separation. *Molecules*, *28*(14). https://doi.org/10.3390/molecules28145293

Coin, Z., Dangwal, S., Irwin, M. H., Knight, T., Bhave, R., Rother, G., Sacci, R., Arifuzzaman, M., Bocharova, V., Ivanov, I., Sholl, D. S., & Islam, S. Z. (2025). Effect of Viscosity of a Deep Eutectic Solvent on CO2 Capture Performance in an Energy-Efficient Membrane Contactor-Based Process. *ACS Omega*, *10*(4), 3407-3417. https://doi.org/10.1021/acsomega.4c06816

Contreras-García, J., Yang, W., & Johnson, E. R. (2011). Analysis of hydrogen-bond interaction potentials from the electron density: integration of noncovalent interaction regions. *J Phys Chem A*, *115*(45), 12983-12990. https://doi.org/10.1021/jp204278k

Dawass, N., Langeveld, J., Ramdin, M., Pérez-Gallent, E., Villanueva, A. A., Giling, E. J. M., Langerak, J., van den Broeke, L. J. P., Vlugt, T. J. H., & Moultos, O. A. (2022). Solubilities and Transport Properties of CO2, Oxalic Acid, and Formic Acid in Mixed Solvents Composed of Deep Eutectic Solvents, Methanol, and Propylene Carbonate. *The Journal of Physical Chemistry B*, *126*(19), 3572-3584. https://doi.org/10.1021/acs.jpcb.2c01425

Desiraju, G. R., & Steiner, T. (2001). *The weak hydrogen bond: in structural chemistry and biology* (Vol. 9). International Union of Crystal.

Elhamarnah, Y., Qiblawey, H., & Nasser, M. (2024). A review on Deep eutectic solvents as the emerging class of green solvents for membrane fabrication and separations. *Journal of Molecular Liquids*, *398*, 124250. https://doi.org/https://doi.org/10.1016/j.molliq.2024.124250

Filonchyk, M., Peterson, M. P., Zhang, L., Hurynovich, V., & He, Y. (2024). Greenhouse gases emissions and global climate change: Examining the influence of CO2, CH4, and N2O. *Science of The Total Environment*, *935*, 173359. https://doi.org/https://doi.org/10.1016/j.scitotenv.2024.173359

Fleming, I. (2011). *Molecular orbitals and organic chemical reactions*. John Wiley & Sons.

Gadre, S. R., Suresh, C. H., & Mohan, N. (2021). Electrostatic Potential Topology for Probing Molecular Structure, Bonding and Reactivity. *Molecules*, *26*(11), 3289. https://doi.org/10.3390/molecules26113289

Geweda, A. E., Zayed, M. E., Khan, M. Y., & Alquaity, A. B. S. (2025). Mitigating CO2 emissions: A review on emerging technologies/strategies for CO2 capture. *Journal of the Energy Institute*, *118*, 101911. https://doi.org/https://doi.org/10.1016/j.joei.2024.101911

Hack, J., Maeda, N., & Meier, D. M. (2022). Review on CO2 Capture Using Amine-Functionalized Materials. *ACS Omega*, *7*(44), 39520-39530. https://doi.org/10.1021/acsomega.2c03385

Hanwell, M. D., Curtis, D. E., Lonie, D. C., Vandermeersch, T., Zurek, E., & Hutchison, G. R. J. J. o. c. (2012). Avogadro: an advanced semantic chemical editor, visualization, and analysis platform. *4*(1), 17.

Hayyan, M., Hashim, M. A., Hayyan, A., Al-Saadi, M. A., AlNashef, I. M., Mirghani, M. E. S., & Saheed, O. K. (2013). Are deep eutectic solvents benign or toxic? *Chemosphere*, *90*(7), 2193-2195. https://doi.org/https://doi.org/10.1016/j.chemosphere.2012.11.004

Humphrey, W., Dalke, A., & Schulten, K. (1996). VMD: Visual molecular dynamics. *Journal of Molecular Graphics*, *14*(1), 33-38. https://doi.org/https://doi.org/10.1016/0263-7855(96)00018-5

Ismael, M., Sahnoun, R., Suzuki, A., Koyama, M., Tsuboi, H., Hatakeyama, N., Endou, A., Takaba, H., Kubo, M., Shimizu, S., Del Carpio, C. A., & Miyamoto, A. (2009). A DFT study on the carbamates formation through the absorption of CO2 by AMP. *International Journal of Greenhouse Gas Control*, *3*(5), 612-616. https://doi.org/https://doi.org/10.1016/j.ijggc.2009.04.002

Ismail, M. F. H., Masri, A. N., Mohd Rashid, N., Ibrahim, I. M., Mohammed, S. A. S., & Yahya, W. Z. N. (2024). A review of CO2 capture for amine-based deep eutectic solvents. *Journal of Ionic Liquids*, *4*(2), 100114. https://doi.org/https://doi.org/10.1016/j.jil.2024.100114

Johnson, E. R., Keinan, S., Mori-Sánchez, P., Contreras-García, J., Cohen, A. J., & Yang, W. (2010). Revealing Noncovalent Interactions. *Journal of the American Chemical Society*, *132*(18), 6498-6506. https://doi.org/10.1021/ja100936w

Książek, E. (2024). Citric Acid: Properties, Microbial Production, and Applications in Industries. *Molecules*, *29*(1), 22. https://www.mdpi.com/1420-3049/29/1/22

Lemaoui, T., Boublia, A., Lemaoui, S., Darwish, A. S., Ernst, B., Alam, M., Benguerba, Y., Banat, F., & AlNashef, I. M. (2023). Predicting the CO2 Capture Capability of Deep Eutectic Solvents and Screening over 1000 of their Combinations Using Machine Learning. *ACS Sustainable Chemistry & Engineering*, *11*(26), 9564-9580. https://doi.org/10.1021/acssuschemeng.3c00415

Leron, R. B., Caparanga, A., & Li, M.-H. (2013). Carbon dioxide solubility in a deep eutectic solvent based on choline chloride and urea at T=303.15–343.15K and moderate pressures. *Journal of the Taiwan Institute of Chemical Engineers*, *44*(6), 879-885. https://doi.org/https://doi.org/10.1016/j.jtice.2013.02.005

Leron, R. B., & Li, M.-H. (2013). Solubility of carbon dioxide in a eutectic mixture of choline chloride and glycerol at moderate pressures. *The Journal of Chemical Thermodynamics*, *57*, 131-136. https://doi.org/https://doi.org/10.1016/j.jct.2012.08.025

Lu, T., & Chen, F. J. J. o. c. c. (2012). Multiwfn: A multifunctional wavefunction analyzer. *33*(5), 580-592.

Luo, F., Liu, X., Chen, S., Song, Y., Yi, X., Xue, C., Sun, L., & Li, J. (2021). Comprehensive Evaluation of a Deep Eutectic Solvent Based CO2 Capture Process through Experiment and Simulation. *ACS Sustainable Chemistry & Engineering*, *9*(30), 10250-10265. https://doi.org/10.1021/acssuschemeng.1c02722

Ma, J., Wang, Y., Yang, X., Zhu, M., & Wang, B. (2021). DFT Study on the Chemical Absorption Mechanism of CO(2) in Diamino Protic Ionic Liquids. *J Phys Chem B*, *125*(5), 1416-1428. https://doi.org/10.1021/acs.jpcb.0c08500

Martínez, L., Andrade, R., Birgin, E., & Martínez, J. M. (2009). PACKMOL: A package for building initial configurations for molecular dynamics simulations. *Journal of Computational Chemistry*, *30*, 2157-2164. https://doi.org/10.1002/jcc.21224

Mohan, M., Demerdash, O., Simmons, B. A., Smith, J. C., K. Kidder, M., & Singh, S. (2023). Accurate prediction of carbon dioxide capture by deep eutectic solvents using quantum chemistry and a neural network [10.1039/D2GC04425K]. *Green Chemistry*, *25*(9), 3475-3492. https://doi.org/10.1039/D2GC04425K

Mohan, M., Demerdash, O. N., Simmons, B. A., Singh, S., Kidder, M. K., & Smith, J. C. (2024). Physics-Based Machine Learning Models Predict Carbon Dioxide Solubility in Chemically Reactive Deep Eutectic Solvents. *ACS Omega*, *9*(17), 19548-19559. https://doi.org/10.1021/acsomega.4c01175

Nandi, R., Paul, N., & Banerjee, T. (2025). Molecular Dynamics Insights of CO2 Capture through Phosphonium-Based Deep Eutectic Solvents for Direct Air Capture. *ACS Sustainable Chemistry & Engineering*, *13*(22), 8234-8248. https://doi.org/10.1021/acssuschemeng.4c10594

National Center for Biotechnology, I. (2026). PubChem Compound Summary for CID 109024, N-Methylmorpholine. *PubChem*. https://pubchem.ncbi.nlm.nih.gov/compound/109024

Neese, F. J. W. I. R. C. M. S. (2025). Software update: The ORCA program system—version 6.0. *15*(2), e70019.

Ortega, J., Lewis, J. P., & Sankey, O. F. (1997). First principles simulations of fluid water: The radial distribution functions. *The Journal of Chemical Physics*, *106*(9), 3696-3702. https://doi.org/https://doi.org/10.1063/1.474121

Paiva, A., Craveiro, R., Aroso, I., Martins, M., Reis, R. L., & Duarte, A. R. C. (2014). Natural Deep Eutectic Solvents – Solvents for the 21st Century. *ACS Sustainable Chemistry & Engineering*, *2*(5), 1063-1071. https://doi.org/10.1021/sc500096j

Parr, R. G. (1989). Density functional theory of atoms and molecules. Horizons of Quantum Chemistry: Proceedings of the Third International Congress of Quantum Chemistry Held at Kyoto, Japan, October 29-November 3, 1979,

Pelaquim, F. P., Barbosa Neto, A. M., Dalmolin, I. A. L., & Costa, M. C. d. (2021). Gas Solubility Using Deep Eutectic Solvents: Review and Analysis. *Industrial & Engineering Chemistry Research*, *60*(24), 8607-8620. https://doi.org/10.1021/acs.iecr.1c00947

Rocha, M., Di Santo, A., Arias, J. M., Gil, D. M., & Altabef, A. B. (2015). Ab-initio and DFT calculations on molecular structure, NBO, HOMO–LUMO study and a new vibrational analysis of 4-(Dimethylamino) Benzaldehyde. *Spectrochimica Acta Part A: Molecular and Biomolecular Spectroscopy*, *136*, 635-643. https://doi.org/https://doi.org/10.1016/j.saa.2014.09.077

Smith, E. L., Abbott, A. P., & Ryder, K. S. (2014). Deep Eutectic Solvents (DESs) and Their Applications. *Chemical Reviews*, *114*(21), 11060-11082. https://doi.org/10.1021/cr300162p

Suresh, C. H. (2022). Molecular electrostatic potential analysis: A powerful tool to interpret and predict chemical reactivity and understand chemical properties of molecules. *WIREs Computational Molecular Science*, *12*(1), e1601. https://doi.org/10.1002/wcms.1601

Xin, K., & van Sint Annaland, M. (2023). Diffusivities and solubilities of carbon dioxide in deep eutectic solvents. *Separation and Purification Technology*, *307*, 122779. https://doi.org/https://doi.org/10.1016/j.seppur.2022.122779

Zhan, C.-G., Nichols, J. A., & Dixon, D. A. (2003). Ionization Potential, Electron Affinity, Electronegativity, Hardness, and Electron Excitation Energy: Molecular Properties from Density Functional Theory Orbital Energies. *The Journal of Physical Chemistry A*, *107*(20), 4184-4195. https://doi.org/10.1021/jp0225774

Zhang, G., Liu, J., Qian, J., Zhang, X., & Liu, Z. (2024). Review of research progress and stability studies of amine-based biphasic absorbents for CO2 capture. *Journal of Industrial and Engineering Chemistry*, *134*, 28-50. https://doi.org/https://doi.org/10.1016/j.jiec.2024.01.013

Zhang, W., Ma, Z., Liu, X., Liu, Y., Hou, Z., Qi, J., Ma, Y., Wang, L., & Wang, Y. (2021). Molecular Mechanism and Absorption Performance Evaluation of CO2 Capture from the PCC Process by Monoethanolamine-Based Deep Eutectic Solvents. *Industrial & Engineering Chemistry Research*, *60*(3), 1483-1493. https://doi.org/10.1021/acs.iecr.0c04970